

Investigation of the corrosion cracks in a C4 heavy transport pipeline by microscopy, fluorescence and diffraction techniques

C. PREDESCU, C. PANTILIMON, M. SOHACIU*, E. MATEI, D. SAVASTRU^a, A. BERBECARU, A. PREDESCU, M.G. ANTON, G. COMAN

Politehnica University of Bucharest, 313 Splaiul Independentei Street, 060042, Romania

^aNational Institute of R&D for Optoelectronics INOE 2000, 409 Atomistilor Street, PO BOX MG-5, RO 077125, Magurele – Ilfov, Romania

The study presents the results of a research performed in order to establish the conditions that lead to the corrosion of a transport pipeline for C4 heavy fraction.

The research includes analysis on the sample collected from the cracked pipeline. The following advanced methods and investigation techniques were used:

- Optical microscopy
- Scanning electron microscopy (SEM)
- X-ray diffraction
- X-ray fluorescence

(Received July 11, 2016; accepted September 29, 2016)

Keywords: Corrosion cracking, Basic medium, Mechanical strain, Microscopy, X-ray diffraction, X-ray fluorescence

1. Introduction

Internal corrosion of a pipeline depends on the composition of the material flowing through it, temperature, pressure and flow regime.[1]

C4 chemistry is based on the cracking of naphtha or of heavier fractions such as crude oils. The C4 hydrocarbons that can be obtained are: n-Butane, i-Butane, n-Butene, i-Butene, Butadiene, Butyne and Vinylacetylene [2].

The bulk properties of a crude assay include specific gravity, sulfur content, nitrogen content, metal (Ni, V, Fe etc.) content, asphalt content, C/H ratio, pour point, flash point, freeze point, smoke point, aniline point, cloud point, viscosity, carbon residue, light hydrocarbon yields (C1–C4), acid number, refractive index and boiling point curve. Bulk properties provide a quick understanding of the type of the oil sample such as sweet and sour, light and heavy etc. However, refineries require fractional properties of the oil sample that reflect the property and composition for specific boiling point range to properly refine it into different end products such as gasoline, diesel and raw materials for chemical processes. Fractional properties usually contain paraffin, naphthenic and aromatics (PNA) compounds, sulfur content, nitrogen content for each boiling-point range, octane number for gasoline, freezing point, cetane index and smoke point for kerosene and diesel fuels [3].

Corrosion in oilfields occurs at all stages from downhole to surface equipment and processing facilities. It appears as leaks in tanks, casings, tubing, pipelines, and other equipment [4-6]. In the petroleum industry, general

and localized corrosion are the most common types of corrosion occurrences. The other large problem in operating pipe flow lines is the internal corrosion [7], mainly due to stress corrosion cracking.

Various protective coatings can be applied in order to reduce or stop the corrosion of the metal, such as, lacquer coatings, slushing compounds, polymeric coatings, sulfonate-base coatings and rust passivators [1].

During the production of steel parts, the deformability of the material is tested through the use of an optimal heating rate and temperature range, specific for each metal or alloy. A high deformation temperature can result in excessive grain growth and oxidation of intercrystalline gaps, which can facilitate the formation of microcracks and subsequently the breach of the wall of the steel part [8, 9, 10].

In this study, the corrosion of a Grade A steel pipe that transported a heavy C4 fraction, is studied by the use of optical microscopy, SEM (Quanta 450 FEG, FEI, USA), EDS, XRF(S8 Tiger, Bruker, USA) and hardness testing. The pipe composition and characteristics are compared to those presented in the ASTM A53 standard for grade A steel pipes.

2. Experimental procedure

The experimental research was done on a sample collected from the area in which the crack occurred, from a pipe that was used for heavy C4 fraction transport. The study follows the pipelines material composition analysis

as well as the analysis of the deposits found on the inside with the purpose to evaluate the processes that lead to the damage on the integrity of the pipe.

The working parameters of the pipeline were a pressure of 12.3 bar and a temperature of 149°C.

For a thorough analysis, the following procedures were used to determine the characteristics of the material and of the crack:

- Visual microscopy analysis.
- Optical (BX 51 M, Olympus, USA) and scanning electron microscopy on the area where the fissure appeared and on the material next to the fissure.
- Material investigation using microanalysis through X-ray (X'Pert PRO MPD, PANalytical, Netherlands) and energy dispersion (EDS) in order to determine the microcomposition.
- XRF analysis on the deposited material.

The 100 mm crack was situated next to a welding joint, which was connected to an elbow fitting (Fig. 1). After opening the pipe, a gelatinous mass, which covered approximately 40% of the lower interior part of the pipe, was observed (Fig. 2).



Fig. 1. Detail view of the area in which the product pipeline cracked



Fig. 2. The appearance of the interior of the pipe after opening

The general aspect of the pipe was deemed technically normal. On the exterior side it showed a thin layer of oxide without any unacceptable imperfections. On the interior, the surface showed general signs of corrosion in points of low intensity (Fig. 3).



Fig. 3. Interior surface of the pipe in the cracked area

The seamless pipe was elaborated out of Grade A material with the following dimensions $\text{Ø } 406.4 \times 9.52$ mm according to ASTM A 53. The wall thickness values measured through non-destructive methods were between 8.7 and 9.3 mm, which are over the minimum allowed thickness of 8.06 mm.

The pipe was examined in terms of chemical composition by use of XRF, the breaking points were analyzed through optical microscopy, SEM and EDS and the sludge found on the inside of the pipeline was also examined through XRF and XRD in order to determine the content of corrosive elements that might have damaged the structural integrity of the pipe.

3. Results and Discussion

3.1. Analysis of pipeline sample

The pipe sample received for analysis presented the dimensions $10 \times 400 \text{ mm} \times 140$.

The chemical composition of the sample obtained through XRF analysis is presented in Table 1.

Table 1. Chemical composition of the pipe material

	Content(%)				
	C	Si	Mn	P	S
Grade A material	≤ 0.25	-	≤ 1.2	≤ 0.05	≤ 0.045
Analyzed sample	0.203	0.196	0.78	0.008	0.023
	Cu	Ni	Cr	Mo	V
	Grade A material	≤ 0.4	≤ 0.4	≤ 0.4	≤ 0.15
Analyzed sample	0.05	0.037	≤ 0.001	0.298	≤ 0.001

The pipe material appears to pertain to the Grade A material specifications with the exception of Mo content, which is 0.3% instead of the maximum allowed of 0.15%.

The microstructure of the material was examined in cross-section relative to the axis of the pipe. A typical aspect is shown in Figure 4.

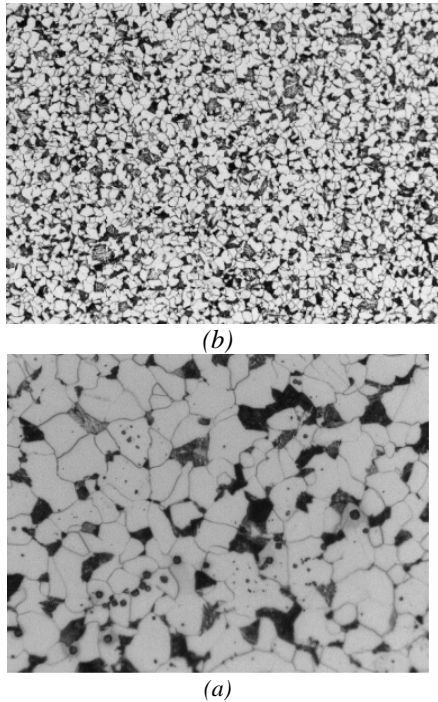


Fig. 4. The microstructure of the pipe material. Attack with NITAL 2%. a) $\times 100$; $\times 500$

The material microstructure consists of ferrite and pearlite with rare areas of overheating structure. These are typical characteristics of the microstructure of a carbon steel in hot rolled condition. ASTM A 53 specifies that pipes must be made by hot rolling, followed by cold calibration in order to ensure employment in shape, dimensions and properties included in the standard.

Strength characteristics prescribed for Grade A material show a hardness of ≥ 96 and the mean measured values on the submitted sample in case of hardness (HV10) were approximately 141.8.

The hardness values found confirm an appropriate level of resistance of the material and together with the microstructural examination results, they support the assessment that the pipe material comes under ASTM A 53 Grade A quality.

After macroscopic examination of the rupture zone, the following aspects have been observed:

- The breaking surface is strongly uneven, cracking fronts were independently developed. During the growth of the fissures depth, they were united in a single front that crossed the pipe wall;

- Morphology of the fracture surfaces shows that the cracking started from the inner surface of the resistance wall and propagated in the thickness direction until its piercing;

- There were no signs of plastic deformation on the edge of the break, which show that the fracture was brittle in nature, and that it was produced under a rated voltage lower than the yield strength of the material.

Microscopic examination revealed the following aspects:

- un-attacked, the pipe wall section appears pierced by fissures mainly oriented towards the thickness direction. The main crack fronts show a tendency to branch out towards smaller fronts nearby (Figure 5)

- after the metallographic attack (Figure 6), the cracking character is obvious, namely to corrosion cracking tension.

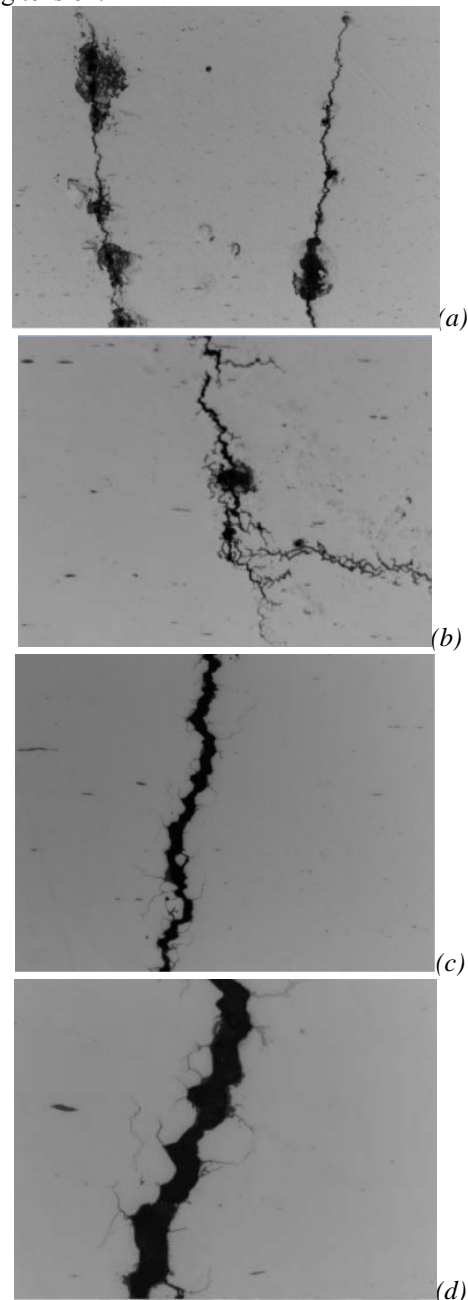


Fig. 5. Un-attacked sample. Cracks in the direction of pipe wall thickness. a, b, c - the sample surface area examined in thickness $\times 200$; c area at $\times 500$

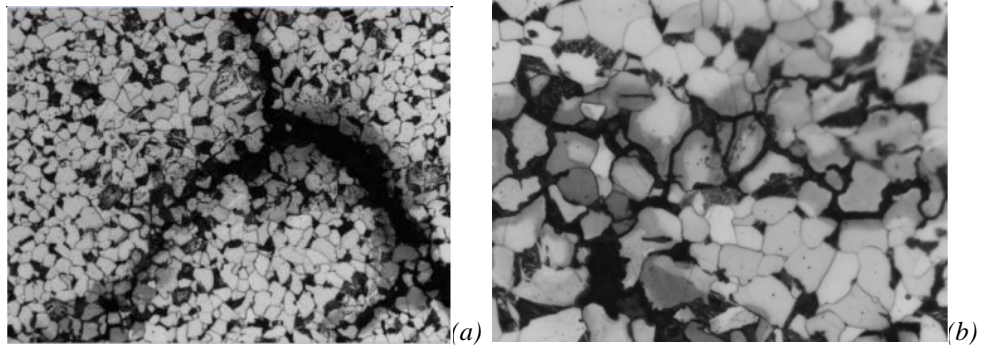
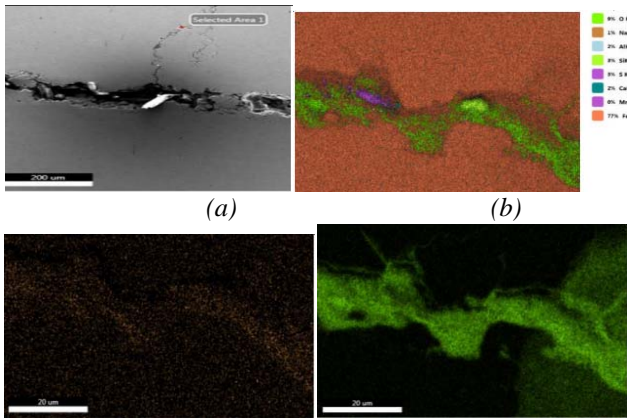
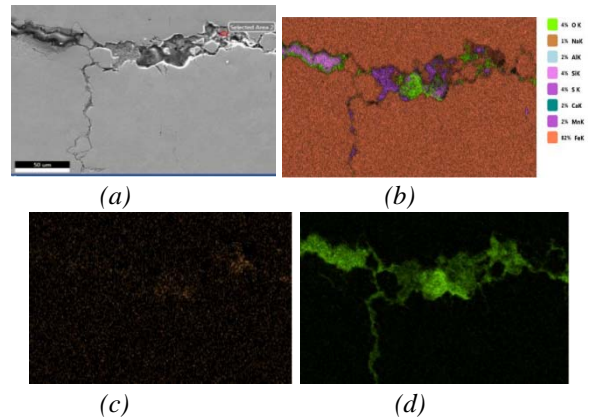


Fig. 6. Sample attacked with NITAL 2%. Details of the cracked areas. a) $\times 200$; b) $\times 500$



Element	Weight %	Atomic %
OK	27,18	52,12
NaK	3,65	4,87
AlK	0,12	0,13
SiK	3,65	3,99
SK	6,86	6,57
CaK	0,6	0,46
MnK	0,6	0,33
FeK	57,33	31,50



Element	Weight %	Atomic %
OK	20,06	46,30
NaK	0,47	0,76
AlK	0,01	0,01
SiK	0,29	0,38
SK	0,20	0,23
CaK	0,30	0,27
MnK	1,15	0,77
FeK	77,52	51,26

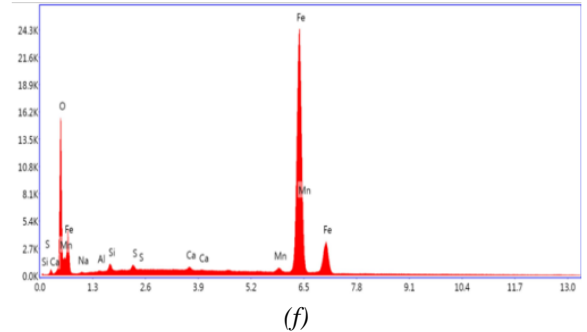
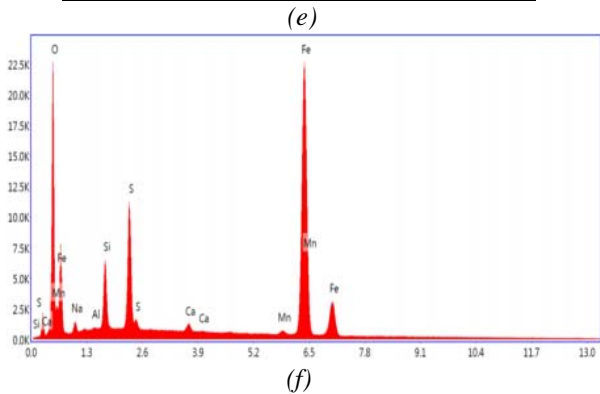


Fig. 7. Image analysis of an area in the crack. a) analyzed area; b) distribution section of various elements; c) the distribution sodium; d) the distribution of oxygen; e) table with elements identified in the spectrogram; f) the spectrogram

Fig. 8. Image analysis of a secondary area in the crack. a) analyzed area; b) distribution section of various elements; c) the distribution sodium; d) the distribution of oxygen; e) table with elements identified in the spectrogram; f) the spectrogram.

After examining the environment of the crack faces by scanning microscopy, the following information was obtained:

- The chemical environment present at crack tips was rich in oxygen, sodium and sulfur;

- Around the finest peaks of the cracks, the presence of an oxygen rich aggressive environment is particularly noticeable.

3.2. Analysis of the material deposited on the inside of the pipe

Qualitative nature of the deposit was evaluated by X-ray fluorescence technique. Prior to analysis, the deposit was washed with water. The result is given in Table 2.

Table 2. The result of X-ray fluorescence analysis on the deposition.

Content (%)				
Fe	Na	S	Al	Si
58.56	15.88	7.43	1.38	0.71
Ca	Mn	Mg	P	Residue
0.44	0.44	0.17	0.06	14.93

The deposition was also analyzed by X-ray diffraction technique and the nature and proportions of the compounds identified are presented in Fig. 9.

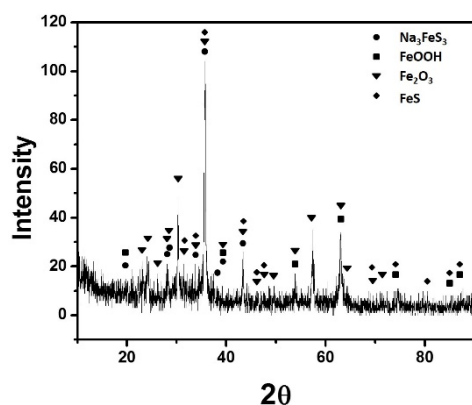


Fig. 9. X-Ray diffraction analysis of the deposition

The material provided for the pipe was unalloyed steel ASTM A53 Grade A. The checks, carried out on the body of evidence extracted from the pipeline, confirmed that the material adhered to the project requirements. Deviation found in the residual content of Mo cannot be traced to the technical incident that occurred.

In the process, the pipeline operated at 85°C and a pressure of 9 bar. In the area of the incident, a relatively consistent deposit was formed inside the pipeline.. Compared to the normal operation of the pipeline, the deposit represents a foreign body. The analysis presented in this report shows that the nature of the deposition compounds indicates high contents of Na, O and S, with a strong basic pH index.

4. Conclusions

The analysis of sample material taken from pipeline confirmed that it corresponded to the material provisions of the Grade A ASTM A 53 quality requirements.

The deviation found in the residual content of Mo cannot be traced to the technical incident.

The cracking of the pipe wall was generated by a process of corrosion energized cracking and had a fragile character, that occurred under a rated voltage lower than the yield strength of the material. In that area, the wall of the pipe presented numerous cracks oriented towards the resistance wall thickness. Analysis carried out by electron microscopy showed that the chemical environment present at the crack tips was rich in oxygen, sodium and sulfur.

Analysis of the deposit was performed by X-ray fluorescence and showed significant contents of Na and S, and the X-ray diffraction analysis revealed compounds rich in Na and S. The deposition, totally void of organic products, indicated a strongly basic pH with a value of 12.

Literature data indicates that non-alloy steel is susceptible to corrosion cracking in strong basic environments. The risk of cracking because of NaOH is present in temperatures over 50°C and it increases with the concentration of NaOH solution and the mechanical strain. The presence in the cracking front of significant concentrations of Na and S leaves no doubt about the decisive importance of the environment in the interior of the pipeline in the corrosion process that lead to the cracking of the pipe.

Acknowledgement

The work has been funded by the Increase of Economic Competitiveness Program through the Financial Agreement ID Project: 1799 / 2015, SMIS 48589

References

- [1] L. Garverick, Corrosion in the Petrochemical Industry, ASM International (1994)
- [2] J Schulze, M. Homann, C4-Hydrocarbons and Derivatives: Resources, Production, Marketing, Springer-Verlag Berlin Heidelberg (1989)
- [3] A.-F. Chang, K. Pashikanti, Y. A. Liu, Refinery Engineering: Integrated Process Modeling and Optimization, Wiley-VCH Verlag GmbH & Co. KGaA (2012)
- [4] M.M. Osman, M.N. Shalaby, Mater. Chem. Phys. **77**, 261 (2003).
- [5] P.C. Okafor, X. Liu, Y.G. Zheng, Corros. Sci. **51**, 761 (2009).
- [6] S. Nešić, W. Sun, in: Tony J.A. Richardson (Ed.), Shreir's Corrosion, Elsevier, Oxford, 1270 (2010)
- [7] S. Ghareba, S. Omanovic, Corros. Sci. **52**, 2104 (2010).
- [8] I. Vida – Simiti, J. Optoelectron. Adv. M. **8**(4), 1479 (2006).
- [9] C. R. Iordanescu, D. Tenciu, I.D. Feraru, A. Kiss, M. Bercu, D. Savastru, R. Notonier, C.E.A. Grigorescu, Dig J Nanomater Bios **6**(2), 863 (2011).
- [10] C.P. Lungu, C.E.A. Grigorescu, I. Jepu, C. Porosnicu, A.M. Lungu, D. Savastru, I.D. Feraru, Diam Relat Mater. **20**, 1061 (2011).